Applied and Computational Mechanics 7 (2013) 205–222

Torsional vibration analysis of shafts based on Adomian decomposition method

R. Tabassian[a,*]

[a] *Department of Mechanical Engineering, Ferdowsi University of Mashhad, Mashhad, Iran*

Received 15 April 2013; received in revised form 6 December 2013

Abstract

In this paper free torsional vibration of shafts is studied using a new approach of solving differential equations called Adomian decomposition method (ADM). Applying this method to free torsional vibration of shafts means a systematic and straightforward procedure for calculating both low and high frequency modes. In this paper different boundary conditions are applied to both end of the shaft and first five natural frequencies and mode shapes are calculated for four different cases. Obtained results are compared with results presented in literature. These results demonstrate that ADM is a suitable approach for analysis of free torsional vibration of shafts which provides precise results with high order of accuracy.

Keywords: Adomian decomposition method, torsional vibration, natural frequencies, shafts, differential equations

1. Introduction

Rotating shafts are extensively implemented for power transmission in different industries. Most machinery may encounter torsional vibration in their rotary elements. Such vibrations could be caused by environmental shocks, random exciting torque, disturbance of electricity or interaction of different parts of system like shafts and bearings. However, the most common type of vibration which occurs in rotary systems is torsional vibration of elements due to resonance phenomenon. In such case, vibration amplitudes may grow quickly to an unacceptable value, by approaching rotational speed to the natural frequencies of system. The demands for higher operational speeds have been increased and resonance instability in such speeds can lead to drastic accidents. Therefore, accurate prediction of natural frequencies is completely crucial for a successful design of rotary systems and free vibrations analysis of shafts is the main problem in the area of rotary dynamics. Importance of this problem has persuaded many researchers to work on this field [1–4]. The most important part of solving a vibration problem is the mathematical modelling. Calculations based on mathematical models, whether complex or simple, can be of value in design, development and fault diagnosis in machines. Although, for solving governing equation of motion of simple shafts, some analytical models have been presented, they are not capable of solving more complicated problems [5]. By development of computers, numerical methods like FEM, FDM or BEM were also developed which are efficiently capable of solving complex problems [6]. However, these methods are not accurate and do not give the exact results. The natural frequencies and the mode shapes obtained from such method are approximate. This inaccuracy is more evident in high natural frequencies and mode shapes which refers to discretisation of problem object.

*Corresponding author. Tel.: +98 935 212 52 71, e-mail: rassoul.tabassian@gmail.com.

In this study a new approach called Adomian Decomposition Method (ADM) is applied to solve torsional vibration of shafts with high order of accuracy in both low and high natural frequencies. ADM was first presented by George Adomian in the early 1980s [7–9]. This method was applied to solve linear and nonlinear initial/boundary-value problems in physics [10]. Lots of reviews and modifications have been done on this approach [11, 12]. The ADM has been receiving much attention in recent years in the area of series solutions. A considerable research work has been devoted recently to this method in order to solve wide class of linear and nonlinear equations [13, 14]. It has been found that, unlike other series solution methods, ADM is easy to program in engineering problems, and provides immediate and visible solution terms without linearisation and discretisation. However, it has not extended in engineering problems properly except a few works. Lai et al. [15] investigated vibration of Euler-Bernoulli beams with different boundary conditions using Adomian decomposition method. Farshidianfar et al. [16] solved free vibration of stepped beam using ADM. They investigated a beam with different cross-sections and also different materials in the step point and obtained natural frequencies and mode shapes of the beam.

In this work we tried to deal with free vibration problem of shafts taking advantage of ADM. Firstly, equations of motion of the shaft is written. Then by substituting series instead of rotational displacement and applying the ADM, recursive relations for the terms of series are obtained. A two-term polynomial with unknown coefficients is considered as the first term of recursive relations. By employing this polynomial in recursive relations, all terms of series are calculated. Applying boundary conditions at both ends of the shaft, a homogeneous system of equations is obtained. A characteristic equation for natural frequencies is obtained by setting the determinant of coefficient matrix to zero. After calculating natural frequencies, mode shapes are also obtained calculating eigenvectors. In order to show capability and accuracy of this method, obtained results are compared with analytical results of other researchers. Unlike FEM and other numerical methods, calculated frequencies by ADM are in precise agreement with analytical solution. Expanding this method to further vibration problems can lead to establishing a powerful exact method in the area of free vibration analysis.

2. Solution Method

2.1. Adomian Decomposition Method

In this section, ADM for solving linear differential equations is briefly explained. Consider the equation

$$Fy = g(x), \tag{1}$$

in which F is a general differential operator that contains derivatives with different orders and $g(x)$ is a specific function. Fy could be decomposed as $Fy = Ly + Ry$ such that L is an invertible operator which contains a highest order of derivatives and R contains reminder order of derivatives. Hence, Eq. (1) can be rewritten as

$$Ly + Ry = g(x)\,. \tag{2}$$

Solving for Ly, one can obtain

$$y = \psi + L^{-1}g - L^{-1}Ry\,. \tag{3}$$

In Eq. (3), ψ is the constant of integral such that $L\psi = 0$. For solving Eq. (3) by ADM, y can be written as series

$$y = \sum_{k=0}^{\infty} y_k. \tag{4}$$

Substituting Eq. (4) into Eq. (3) yields

$$\sum_{k=0}^{\infty} y_k = \psi + L^{-1}g - L^{-1}R \sum_{k=0}^{\infty} y_k. \tag{5}$$

In above equation by assuming $y_0 = \psi + L^{-1}g$, the recursive formula is obtained as follows:

$$y_k = -L^{-1}Ry_{k-1}, \qquad k \geq 1. \tag{6}$$

In practice all terms of series cannot be determined exactly, however the solutions can only be approximated by a truncated series $y = \sum_{k=0}^{n-1} y_k$ [7].

2.2. *Applying ADM to Free Vibration Formulation of Shafts*

The circular shaft shown in Fig. 1a is considered. Fig. 1b illustrates a differential segment of the shaft with length $\mathrm{d}x$ for which all internal torsional moment and deformations are displayed. In this figure T represents torsional moment and θ denotes angular displacement. The equation of motion of shaft is written using the equilibrium equation of the internal moments acting on differential segment

$$\left(T + \frac{\partial T}{\partial x}\,\mathrm{d}x\right) - T = \rho I_p \,\mathrm{d}x\, \frac{\partial^2 \theta}{\partial t^2}, \tag{7}$$

where I_p is polar moment of inertia of cross section and ρ is density of the shaft material. Substituting $T = I_p G(\partial\theta/\partial x)$ in Eq. (7) and considering $I_p G$ constant, one can obtain

$$\frac{\partial^2 \theta(x,t)}{\partial x^2} = \frac{1}{c^2}\,\frac{\partial^2 \theta(x,t)}{\partial t^2}, \tag{8}$$

where $c^2 = G/\rho$ and G is shear modulus of the shaft.

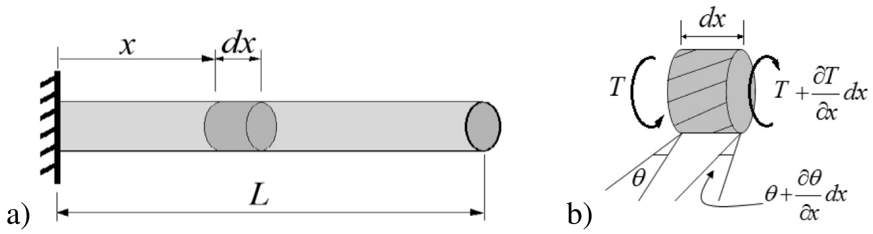

Fig. 1. (a) Circular shaft, (b) Internal torsional moment and deformations of a differential segment of the shaft

In Eq. (8), $\theta(x,t)$ can be separated into two functions

$$\theta(x,t) = \Phi(x)q(t), \tag{9}$$

where $\Phi(x)$ is modal displacement and $q(t)$ is a harmonic function of time. If ω denotes the frequency of $q(t)$ then

$$\frac{\partial^2 \theta(x,t)}{\partial t^2} = -\omega^2 \Phi(x)q(t). \tag{10}$$

By substituting Eq. (9) and (10) into Eq. (8) and eliminating $q(t)$, below differential equation is derived

$$\frac{\mathrm{d}^2\Phi(x)}{\partial x^2} + \frac{\omega^2}{c^2}\,\Phi(x) = 0. \tag{11}$$

This equation could be rewritten in non-dimensional form

$$\frac{\mathrm{d}^2\Phi(X)}{\mathrm{d}X^2} - \lambda\Phi(X) = 0, \tag{12}$$

in which $X = x/l$, $\lambda = -l^2\omega^2/c^2$ and l is length of the shaft. The linear operator L in Eq. (12) is defined as $L\Phi = \mathrm{d}^2\Phi(X)/\mathrm{d}X^2$. Furthermore, angular displacement $\Phi(X)$ can be written as follows:

$$\Phi(X) = \psi + L^{-1}\lambda\Phi(X), \tag{13}$$

where $L^{-1} = \iint \ldots \mathrm{d}X\,\mathrm{d}X$. Assuming $\Phi(X) \approx \sum_{k=0}^{n-1}\varphi_k(X)$ and substituting it into Eq. (13) yields

$$\sum_{k=0}^{n-1}\varphi_k(X) = \psi + \lambda L^{-1}\sum_{k=0}^{n-1}\varphi_k(X). \tag{14}$$

As mentioned before, ψ is constant of integral such that $L\psi = 0$. Also, the first term of left side series is considered equal to $\psi + L^{-1}g$. Since Eq. (12) is a homogenous differential equation, function g does not exist. Therefore,

$$\varphi_0(X) = \psi = \varphi(0) + \varphi'(0)X. \tag{15}$$

Hence, recursive formulae for equations are obtained as:

$$\varphi_k(X) = \lambda\int_0^X\!\!\int_0^X \varphi_{k-1}(X)\,\mathrm{d}X\,\mathrm{d}X \quad \text{for} \quad k \geq 1. \tag{16}$$

By substituting $\varphi_0(X)$ into above recursive formula as first term, and expanding other terms, $\varphi_k(X)$ is obtained

$$\varphi_k(X) = \lambda^k\left(\frac{X^{2k}}{(2k)!}\,\Phi(0) + \frac{X^{2k+1}}{(2k+1)!}\,\Phi'(0)\right). \tag{17}$$

After achieving the general term of series, $\Phi(X)$ can be approximated as follows:

$$\Phi(X) = \sum_{k=0}^{n-1}\lambda^k\left(\frac{X^{2k}}{(2k)!}\,\Phi(0) + \frac{X^{2k+1}}{(2k+1)!}\,\Phi'(0)\right). \tag{18}$$

By applying boundary conditions at the both ends, a homogenous system of equations with two unknown is obtained. Setting determinant of coefficient matrix equal to zero produces a characteristic equation for natural frequencies.

2.3. Boundary Conditions

In this part four common boundary conditions of shafts are discussed. In reality each end of the shaft could have one of these conditions.

Fixed end

Fixed end condition is shown in Fig. 2. In this condition angular displacement is equal to zero ($\theta = 0$).

This condition for the beginning of the shaft could be written as

$$\theta(0, t) = 0 \to \Phi(0) = 0 \tag{19}$$

and similarly, fixed condition at the end of the shaft is written as

$$\theta(l, t) = 0 \to \Phi(1) = 0. \tag{20}$$

Hence,

$$\Phi(1) = \sum_{k=0}^{n-1} \lambda^k \left(\frac{\Phi(0)}{(2k)!} + \frac{\Phi'(0)}{(2k+1)!} \right) = 0. \tag{21}$$

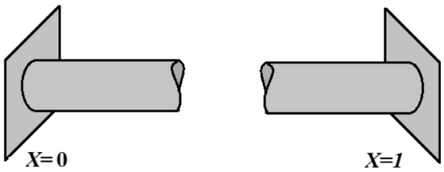

Fig. 2. Fixed end boundary conditions

Free end

Free end condition is shown in Fig. 3. In this condition torsional moment is equal to zero ($T = I_p G(\partial\theta/\partial x) = 0$).

This condition for the beginning of the shaft could be written as

$$\left.\frac{\mathrm{d}\theta(x, t)}{\mathrm{d}x}\right|_{x=0} = 0 \to \Phi'(0) = 0 \tag{22}$$

and similarly, free condition at the end of the shaft is written as

$$\left.\frac{\mathrm{d}\theta(x, t)}{\mathrm{d}x}\right|_{x=l} = 0 \to \left.\frac{\mathrm{d}\Phi(X)}{\mathrm{d}X}\right|_{X=1} = 0. \tag{23}$$

Hence,

$$\left.\frac{\mathrm{d}\Phi(X)}{\mathrm{d}X}\right|_{X=1} = \sum_{k=1}^{n-1} \lambda^k \frac{\Phi(0)}{(2k-1)!} + \sum_{k=0}^{n-1} \lambda^k \frac{\Phi'(0)}{(2k)!} = 0. \tag{24}$$

Fig. 3. Free end boundary conditions

Spring support

Spring support condition is shown in Fig. 4. Torsional moment is proportional to angular displacement ($T = \pm K_T\theta$) in this condition. K_T is torsional spring constant.

This condition for the beginning of the shaft could be written as:

$$I_pG\,\frac{\mathrm{d}\theta(x,t)}{\mathrm{d}x}\bigg|_{x=0} = K_{T0}\theta(0,t) \to K_{T0}\Phi(0) - \frac{I_pG}{l}\,\Phi'(0) = 0 \tag{25}$$

and similarly at the end of the shaft, this condition is written as

$$I_pG\,\frac{\mathrm{d}\theta(x,t)}{\mathrm{d}x}\bigg|_{x=l} = -K_{T1}\theta(l,t) \to K_{T1}\Phi(1) + \frac{I_pG}{l}\,\frac{\mathrm{d}\Phi(X)}{\mathrm{d}X}\bigg|_{X=1} = 0. \tag{26}$$

Hence,

$$K_{T1}\sum_{k=0}^{n-1}\lambda^k\left(\frac{\Phi(0)}{(2k)!} + \frac{\Phi'(0)}{(2k+1)!}\right) + \frac{I_pG}{l}\left(\sum_{k=1}^{n-1}\lambda^k\frac{\Phi(0)}{(2k-1)!} + \sum_{k=0}^{n-1}\lambda^k\frac{\Phi'(0)}{(2k)!}\right) = 0. \tag{27}$$

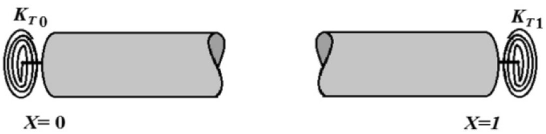

Fig. 4. Spring supported conditions

Concentrated Rotary Mass

In some cases a concentrated rotary mass is added to the end of the shaft which produces rotary inertia at this end. Fig. 5 displays a disk with mass moment of inertia J_i ($i = 0, 1$) added to the ends. Here, moment equilibrium of the disk could be written to obtain equations of this condition

$$\sum M = J\ddot{\theta} \to J_i\,\frac{\partial^2\theta}{\partial t^2} = \pm I_pG\,\frac{\partial\theta}{\partial x} \qquad (i = 0, 1). \tag{28}$$

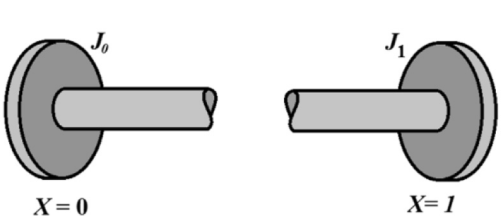

Fig. 5. Shaft with concentrated rotary mass at ends

Substituting Eqs. (9) and (10) into Eq. (28) and eliminating $q(t)$ yields

$$-J_i\omega^2\Phi = \pm\frac{I_pG}{l}\,\frac{\mathrm{d}\Phi}{\mathrm{d}X} \qquad (i = 0, 1). \tag{29}$$

This condition for the beginning of the shaft could be written as

$$J_0\omega^2\Phi(0) + \frac{I_pG}{l}\,\Phi'(0) = 0 \tag{30}$$

and similarly, at the end of the shaft it could be obtained as follows:

$$-J_1\omega^2\Phi(1) + \frac{I_pG}{l}\,\frac{\mathrm{d}\Phi(X)}{\mathrm{d}X}\bigg|_{X=1} = 0. \tag{31}$$

Hence,

$$-J_1\omega^2\sum_{k=0}^{n-1}\lambda^k\left(\frac{\Phi(0)}{(2k)!} + \frac{\Phi'(0)}{(2k+1)!}\right) + \frac{I_pG}{l}\left(\sum_{k=1}^{n-1}\lambda^k\frac{\Phi(0)}{(2k-1)!} + \sum_{k=0}^{n-1}\lambda^k\frac{\Phi'(0)}{(2k)!}\right) = 0. \tag{32}$$

As observed so far, all the boundary conditions lead to homogenous equations which contain unknowns $\Phi(0)$ and $\Phi'(0)$. Every shaft has one of these boundary conditions at each end. Therefore, a homogenous system of equations with two unknowns has to be solved. For non-trivial solution of equations, the determinant of coefficients matrix must be zero. Doing so gives us the characteristic equation for calculating natural frequencies. Most of coefficients are series in which increasing the order of series truncation (n) leads to increasing the number of achievable natural frequencies and enhancing the accuracy of them, as well. In order to reach desired accuracy, n should be increased until below stated relation is satisfied:

$$\left|\Omega_i^n - \Omega_i^{n-1}\right| \le \varepsilon, \tag{33}$$

where Ω_i^n and Ω_i^{n-1} are the i-th estimated eigenvalues corresponding to n and $n-1$ and ε is the order of desired accuracy.

3. Numerical Study

In order to demonstrate the capability and the efficiency of ADM in solving vibration analysis of shafts, four different specific cases are studied in this part. By applying mentioned relations in previous section, one can obtain the natural frequencies of shaft with various boundary conditions at each end. The procedure is coded as computer program to calculate natural frequencies as accurate as possible. Material properties and geometries of the shaft are kept constant for all cases and only boundary conditions are changed. Table 1 shows material properties and geometries of the shaft.

Table 1. Material properties and geometries of the shaft

Length of the shaft (l)	1 000 mm
Radius of cross-section (r)	50 mm
Shear modulus (G)	79.3 GPa
Density (ρ)	7 800 kg/m^3

Non-dimensional parameters of frequency (Ω_n), rotary inertia of concentrated mass (S_0, S_1) and spring constants (R_0, R_1) are defined:

$$\Omega_n = \omega_n\frac{l}{c},$$
$$S_0 = \frac{J_0}{\rho I_p l}, \qquad S_1 = \frac{J_1}{\rho I_p l},$$
$$R_0 = \frac{K_{T0}l}{GI_p}, \qquad R_1 = \frac{K_{T1}l}{GI_p}. \tag{34}$$

Case I : Fixed-Fixed

As first case, the shaft shown in Fig. 6 is considered. This shaft is completely fixed at both ends. Therefore, Eqs. (19) and (21) should be applied

$$\begin{cases} \Phi(0) = 0, \\ \sum_{k=1}^{n-1} \lambda^k \frac{\Phi(0)}{(2k-1)!} + \sum_{k=0}^{n-1} \lambda^k \frac{\Phi'(0)}{(2k)!} = 0. \end{cases} \tag{35}$$

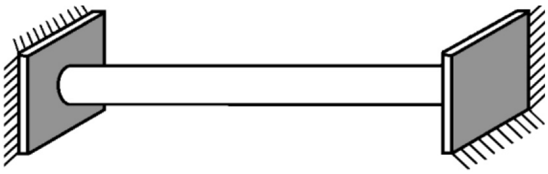

Fig. 6. Fixed-Fixed shaft

For non-trivial solution of this system of equations, determinant of coefficient matrix should be set to zero

$$\begin{vmatrix} 1 & 0 \\ \sum_{k=1}^{n-1} \frac{\lambda^k}{(2k-1)!} & \sum_{k=0}^{n-1} \frac{\lambda^k}{(2k)!} \end{vmatrix} = 0. \tag{36}$$

Natural frequencies of the shaft could be achieved by solving Eq. (36). Table 2 presents the frequencies calculated for different values of n (order of series truncation). As observed in this table by increasing n, number of achievable frequencies and also accuracy of them increase and obtained natural frequencies converge to their exact values.

For torsional vibration of Fixed-Fixed shaft there is an analytical solution [5]. The results calculated by using analytical solution are also mentioned in the last row of Table 2 to be compared with results obtained by ADM. As displayed in Table 2 by choosing $n = 30$, the first five non-dimensional natural frequencies of the shaft with high order of accuracy are obtained.

After calculating natural frequencies, mode shapes are also achievable. By calculating eigenvectors corresponding to each eigenvalue and substituting in Eq. (18), mode shapes of Fixed-Fixed shaft are obtained. Fig. 7 displays calculated mode shapes for this case.

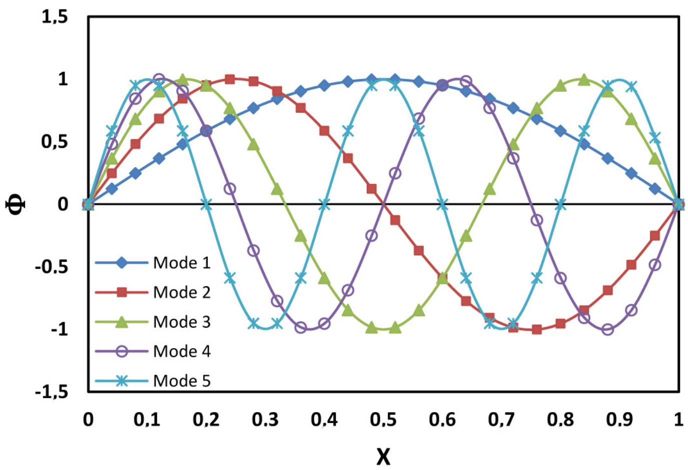

Fig. 7. The first five normalized mode shapes of Fixed-Fixed shaft

Table 2. Five non-dimensional natural frequencies of the fixed-fixed shaft

n	Ω_1	Ω_2	Ω_3	Ω_4	Ω_5
2	2.449 489 743				
3	–				
4	3.078 642 304				
5	3.148 690 071	4.963 152 867			
6	3.141 148 305	–			
7	3.141 613 798	5.978 351 111			
8	3.141 591 881	6.416 050 834	7.105 718 728		
9	3.141 592 676	6.272 546 537	–		
10	3.141 592 653	6.284 237 155	8.607 051 935		
11	3.141 592 654	6.283 102 591	–		
12	3.141 592 654	6.283 190 802	9.324 85 472		
13	3.141 592 654	6.283 184 996	9.442 331 867	10.981 671 75	
14	3.141 592 654	6.283 185 322	9.422 937 801	–	
15	3.141 592 654	6.283 185 307	9.424 956 716	12.129 377 54	
16	3.141 592 654	6.283 185 307	9.424 762 799	–	
17	3.141 592 654	6.283 185 307	9.424 779 101	12.542 375 98	
18	3.141 592 654	6.283 185 307	9.424 777 884	12.569 472 32	14.651 779 32
19	3.141 592 654	6.283 185 307	9.424 777 965	12.566 040 31	–
20	3.141 592 654	6.283 185 307	9.424 777 961	12.566 402 72	15.527 006 35
21	3.141 592 654	6.283 185 307	9.424 777 961	12.566 367 79	15.753 036 23
22	3.141 592 654	6.283 185 307	9.424 777 961	12.566 370 84	15.703 018 48
23	3.141 592 654	6.283 185 307	9.424 777 961	12.566 370 60	15.708 541 47
24	3.141 592 654	6.283 185 307	9.424 777 961	12.566 370 62	15.707 902 27
25	3.141 592 654	6.283 185 307	9.424 777 961	12.566 370 61	15.707 969 21
26	3.141 592 654	6.283 185 307	9.424 777 961	12.566 370 61	15.707 962 73
27	3.141 592 654	6.283 185 307	9.424 777 961	12.566 370 61	15.707 963 31
28	3.141 592 654	6.283 185 307	9.424 777 961	12.566 370 61	15.707 963 26
29	3.141 592 654	6.283 185 307	9.424 777 961	12.566 370 61	15.707 963 27
30	3.141 592 654	6.283 185 307	9.424 777 961	12.566 370 61	15.707 963 27
Gorman[5]	3.141 592 654	6.283 185 307	9.424 777 961	12.566 370 61	15.707 963 27

Case II: Fixed-Concentrated Rotary Mass

In this case as displayed in Fig. 8 a concentrated rotary mass is added to the free end of the shaft.

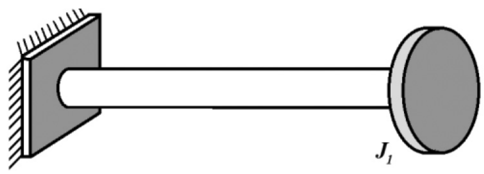

Fig. 8. Fixed-Free shaft with concentrated rotary mass at free end

Concentrated mass rotary inertia at the end of the shaft is $S_1 = 1$. Applying boundary conditions for this shaft leads to below homogenous system of equations

$$\begin{cases} \Phi(0) = 0, \\ J_1\omega^2 \sum_{k=0}^{n-1} \lambda^k \left(\frac{\Phi(0)}{(2k)!} + \frac{\Phi'(0)}{(2k+1)!}\right) + \frac{I_pG}{l}\left(\sum_{k=1}^{n-1} \lambda^k \frac{\Phi(0)}{(2k-1)!} + \sum_{k=0}^{n-1} \lambda^k \frac{\Phi'(0)}{(2k)!}\right) = 0. \end{cases} \tag{37}$$

Non-trivial solution of this system of equations is obtained by setting the determinant of coefficient matrix to zero

$$\begin{vmatrix} 1 & 0 \\ \sum_{k=1}^{n-1} \frac{I_pG}{l} \frac{\lambda^k}{(2k-1)!} + \sum_{k=0}^{n-1} \frac{J_1\omega^2\lambda^k}{(2k)!} & \sum_{k=1}^{n-1} \frac{I_pG}{l} \frac{\lambda^k}{(2k)!} + \sum_{k=0}^{n-1} \frac{J_1\omega^2\lambda^k}{(2k+1)!} \end{vmatrix} = 0. \tag{38}$$

The first five natural frequencies and the corresponding mode shapes calculated for this case are presented in Table 3 and Fig. 9 respectively. As observed in Table 3 by choosing $n = 25$, proper order of accuracy is achieved for the natural frequencies. In this case effects of rotary inertia of concentrated mass on natural frequencies of the shaft are also studied. Table 4 shows frequencies calculated for different values of rotary mass. It could be seen that by increasing rotary inertia at the end of the shaft, natural frequencies decrease.

Table 3. Five non-dimensional natural frequencies of Fixed-Free shaft with concentrated rotary mass at free end ($S_1 = 1$)

n	Ω_1	Ω_2	Ω_3	Ω_4	Ω_5
2	0.851 517 928	2.876 615 584			
3	0.860 573 158	–			
4	0.860 330 327	3.394 367 058			
5	0.860 333 616	3.426 817 116	5.203 408 673		
6	0.860 333 589	3.425 737 707	–		
7	0.860 333 589	3.425 599 900	6.159 194 051		
8	0.860 333 589	3.425 619 779	6.546 823 759	7.290 816 112	
9	0.860 333 589	3.425 618 396	6.428 419 631	–	
10	0.860 333 589	3.425 618 462	6.438 134 110	8.736 254 249	
11	0.860 333 589	3.425 618 459	6.437 235 888	–	
12	0.860 333 589	3.425 618 459	6.437 302 052	9.434 569 641	
13	0.860 333 589	3.425 618 459	6.437 297 977	9.545 654 697	11.084 634 88
14	0.860 333 589	3.425 618 459	6.437 298 188	9.527 635 393	–
15	0.860 333 589	3.425 618 459	6.437 298 179	9.529 497 610	12.216 967 00
16	0.860 333 589	3.425 618 459	6.437 298 179	9.529 320 727	–
17	0.860 333 589	3.425 618 459	6.437 298 179	9.529 335 421	12.622 122 31
18	0.860 333 589	3.425 618 459	6.437 298 179	9.529 334 338	12.648 265 09
19	0.860 333 589	3.425 618 459	6.437 298 179	9.529 334 409	12.644 971 24
20	0.860 333 589	3.425 618 459	6.437 298 179	9.529 334 405	12.645 317 81
21	0.860 333 589	3.425 618 459	6.437 298 179	9.529 334 405	12.645 284 54
22	0.860 333 589	3.425 618 459	6.437 298 179	9.529 334 405	12.645 287 44
23	0.860 333 589	3.425 618 459	6.437 298 179	9.529 334 405	12.645 287 21
24	0.860 333 589	3.425 618 459	6.437 298 179	9.529 334 405	12.645 287 22
25	0.860 333 589	3.425 618 459	6.437 298 179	9.529 334 405	12.645 287 22
Gorman[5]	0.860 333 589	3.425 618 459	6.437 298 179	9.529 334 405	12.645 287 22

Case III: Spring Support at Both Ends

Fig. 10 shows a shaft which is constrained by torsional springs at both ends. Torsional spring constants for constrains are $R_0 = R_1 = 10$. Eqs. (25) and (27) should be applied for boundary conditions:

$$\begin{cases} K_{T0}\Phi(0) - \frac{I_pG}{l}\Phi'(0) = 0, \\ K_{T1}\sum_{k=0}^{n-1}\lambda^k\left(\frac{\Phi(0)}{(2k)!} + \frac{\Phi'(0)}{(2k+1)!}\right) + \frac{I_pG}{l}\left(\sum_{k=1}^{n-1}\lambda^k\frac{\Phi(0)}{(2k-1)!} + \sum_{k=0}^{n-1}\lambda^k\frac{\Phi'(0)}{(2k)!}\right) = 0. \end{cases} \tag{39}$$

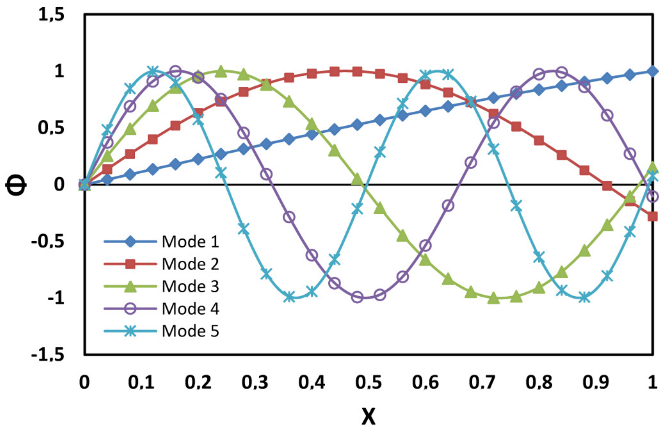

Fig. 9. The first five mode shapes of Fixed-Free shaft with concentrated rotary mass at free end

Table 4. Non-dimensional natural frequencies for different values of rotary mass

S_1	Ω_1	Ω_2	Ω_3	Ω_4	Ω_5
0.01	1.555 245 129	4.665 765 142	7.776 374 078	10.887 13 010	13.998 089 74
0.02	1.540 005 942	4.620 245 731	7.701 159 370	10.783 16 424	13.866 633 36
0.05	1.496 128 952	4.491 480 046	7.495 412 093	10.511 66 997	13.541 976 80
0.1	1.428 870 011	4.305 801 413	7.228 109 772	10.200 26 259	13.214 185 68
0.2	1.313 837 716	4.033 567 790	6.909 595 795	9.892 752 565	12.935 221 28
0.5	1.076 873 986	3.643 597 167	6.578 333 733	9.629 560 343	12.722 298 77
1	0.860 333 589	3.425 618 459	6.437 298 179	9.529 334 405	12.645 287 22
2	0.653 271 187	3.292 310 021	6.361 620 392	9.477 485 705	12.606 013 44
5	0.432 840 720	3.203 935 001	6.314 846 121	9.445 947 898	12.582 264 67
10	0.311 052 848	3.173 097 177	6.299 059 360	9.435 375 976	12.574 323 16
20	0.221 760 394	3.157 427 009	6.291 132 834	9.430 080 093	12.570 348 21
50	0.140 951 676	3.147 945 917	6.286 366 784	9.426 899 546	12.567 961 96
100	0.099 833 639	3.144 772 523	6.284 776 452	9.425 838 874	12.567 166 34

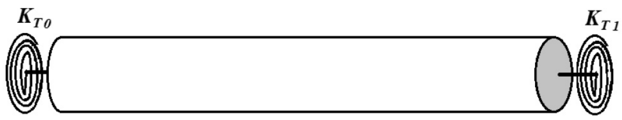

Fig. 10. Shaft with torsional springs at both ends

Non-trivial solution is obtained setting the determinant of coefficient to zero

$$\begin{vmatrix} K_{T0} & -\frac{I_pG}{l} \\ \sum_{k=1}^{n-1} \frac{I_pG}{l}\frac{\lambda^k}{(2k-1)!} + \sum_{k=0}^{n-1} \frac{K_{T1}\lambda^k}{(2k)!} & \sum_{k=1}^{n-1} \frac{I_pG}{l}\frac{\lambda^k}{(2k)!} + \sum_{k=0}^{n-1} \frac{K_{T1}\lambda^k}{(2k+1)!} \end{vmatrix} = 0. \tag{40}$$

Solving Eq. (40) leads to natural frequencies of the shaft which are presented in Table 5. In the last row of Table 5, the results obtained by Rao's [17] for this case are presented to be compared with ADM results. As observed, by increasing the value of n, obtained natural frequencies are converging to constant values and choosing appropriate n provides proper agreement with Rao results. Corresponding mode shape are achieved replacing eigenvectors in Eq. (18). The mode shapes obtained for spring supported shaft are illustrated in Fig. 11.

Table 5. Five non-dimensional natural frequencies of the shaft with symmetric spring supports

n	Ω_1	Ω_2	Ω_3	Ω_4	Ω_5
2	2.082 630 404				
3	–				
4	2.590 311 893				
5	2.631 043 158	4.375 761 700			
6	2.627 496 687	–			
7	2.627 682 451	5.165 133 582			
8	2.627 675 224	5.335 597 438	6.583 034 180		
9	2.627 675 438	5.304 839 307	–		
10	2.627 675 433	5.307 519 740	7.690 710 327		
11	2.627 675 433	5.307 312 380	–		
12	2.627 675 433	5.307 325 461	8.050 383 722		
13	2.627 675 433	5.307 324 769	8.068 997 608	10.129 520 65	
14	2.627 675 433	5.307 324 800	8.066 968 923	–	
15	2.627 675 433	5.307 324 799	8.067 148 604	10.821 490 45	
16	2.627 675 433	5.307 324 799	8.067 134 691	10.923 203 30	12.451 768 64
17	2.627 675 433	5.307 324 799	8.067 135 634	10.907 174 84	–
18	2.627 675 433	5.307 324 799	8.067 135 578	10.908 859 18	13.504 137 52
19	2.627 675 433	5.307 324 799	8.067 135 581	10.908 694 16	13.968 730 04
20	2.627 675 433	5.307 324 799	8.067 135 581	10.908 708 57	13.806 938 14
21	2.627 675 433	5.307 324 799	8.067 135 581	10.908 707 43	13.820 661 81
22	2.627 675 433	5.307 324 799	8.067 135 581	10.908 707 51	13.819 038 29
23	2.627 675 433	5.307 324 799	8.067 135 581	10.908 707 51	13.819 206 26
24	2.627 675 433	5.307 324 799	8.067 135 581	10.908 707 51	13.819 190 31
25	2.627 675 433	5.307 324 799	8.067 135 581	10.908 707 51	13.819 191 69
26	2.627 675 433	5.307 324 799	8.067 135 581	10.908 707 51	13.819 191 58
27	2.627 675 433	5.307 324 799	8.067 135 581	10.908 707 51	13.819 191 59
28	2.627 675 433	5.307 324 799	8.067 135 581	10.908 707 51	13.819 191 59
Rao[17]	2.627675	5.307324	8.067135	10.90871	13.81919

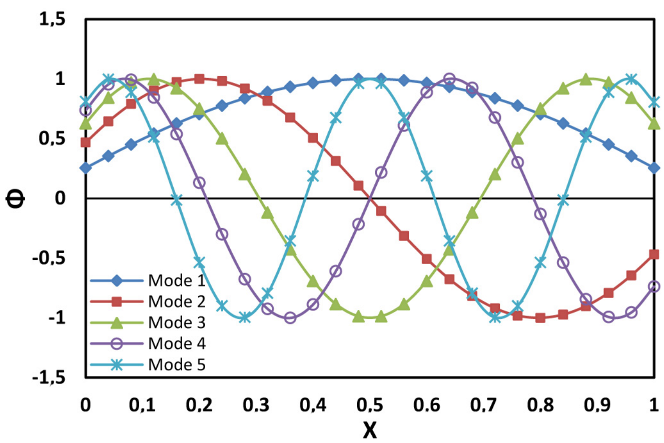

Fig. 11. The first five mode shapes of the shaft with symmetric spring supports

In this case effects of rotational springs on natural frequencies of the shaft are also investigated. Table 6 contains the results obtained for a shaft supported by symmetric springs. It could be observed that by increasing spring constant at the ends natural frequencies approach to the natural frequencies of fixed-fixed shaft (Case I). Table 7 shows the results obtained for a shaft with asymmetric spring supports, i.e. when the spring constant at the beginning is increased, the spring constant at the end of the shaft is reduced. As observed in Table 7, the increase of the spring constant at the left end causes that natural frequencies of the shaft approach to the natural frequencies of Fixed-Free shaft [5].

Table 6. Effects of rotary springs on natural frequencies of the shaft with symmetric spring supports ($R_0 = R_1 = R$)

R	Ω_1	Ω_2	Ω_3	Ω_4	Ω_5
10^{-5}	0.004 472 132	3.141 599 020	6.283 188 490	9.424 780 08	12.566 372 21
5×10^{-5}	0.009 999 958	3.141 624 484	6.283 201 223	9.424 788 57	12.566 378 57
10^{-4}	0.014 142 018	3.141 656 314	6.283 217 138	9.424 799 18	12.566 386 53
5×10^{-4}	0.031 621 459	3.141 910 931	6.283 344 458	9.424 884 06	12.566 450 19
10^{-3}	0.044 717 633	3.142 229 144	6.283 503 601	9.424 990 16	12.566 529 77
5×10^{-3}	0.099 958 352	3.144 772 531	6.284 776 453	9.425 838 87	12.567 166 34
10^{-2}	0.141 303 613	3.147 945 981	6.286 366 792	9.426 899 55	12.567 961 96
5×10^{-2}	0.314 916 173	3.173 104 919	6.299 060 357	9.435 376 27	12.574 323 29
10^{-1}	0.443 520 788	3.203 994 477	6.314 854 018	9.445 950 26	12.582 265 67
5×10^{-1}	0.960 188 874	3.431 014 305	6.438 197 151	9.529 617 83	12.645 409 52
10^{0}	1.306 542 374	3.673 194 406	6.584 620 043	9.631 684 64	12.723 240 78
5×10^{0}	2.284 453 710	4.761 288 969	7.463 676 172	10.326 611 0	13.286 241 50
10^{1}	2.627 675 433	5.307 324 799	8.067 135 581	10.908 707 5	13.819 191 59
5×10^{1}	3.020 903 234	6.042 646 001	9.066 034 201	12.091 809 7	15.120 625 98
10^{2}	3.080 011 884	6.160 138 033	9.240 491 463	12.321 182 7	15.402 318 74
5×10^{2}	3.129 076 511	6.258 153 998	9.387 233 438	12.516 315 8	15.645 402 07
10^{3}	3.135 322 030	6.270 644 183	9.405 966 582	12.541 289 4	15.676 612 61
5×10^{3}	3.140 336 519	6.280 673 039	9.421 009 561	12.561 346 1	15.701 682 62
10^{4}	3.140 964 461	6.281 928 922	9.422 893 383	12.563 857 8	15.704 822 31
5×10^{4}	3.141 466 995	6.282 933 990	9.424 400 985	12.565 868 0	15.707 334 97
10^{5}	3.141 529 823	6.283 059 646	9.424 589 469	12.566 119 3	15.707 649 11
Fixed-Fixed	3.141 592 654	6.283 185 307	9.424 777 961	12.566 370 6	15.707 963 27

Table 7. Effects of rotary springs on natural frequencies of the shaft with asymmetric spring supports

R_0	R_1	Ω_1	Ω_2	Ω_3	Ω_4	Ω_5
10^{0}	10^{0}	1.306 542 374	3.673 194 406	6.584 620 043	9.631 684 636	12.723 240 78
5×10^{0}	0.5×10^{0}	1.573 559 191	4.140 869 227	6.976 567 722	9.941 048 936	12.972 770 72
10^{1}	10^{-1}	1.489 910 837	4.327 111 118	7.241 068 370	10.209 599 60	13.221 483 34
5×10^{1}	0.5×10^{-1}	1.571 194 942	4.630 832 566	7.707 522 144	10.787 712 19	13.870 172 48
10^{2}	10^{-2}	1.561 585 403	4.667 886 271	7.777 647 159	10.888 039 55	13.998 797 14
5×10^{2}	0.5×10^{-2}	1.570 837 666	4.704 044 085	7.838 942 874	10.974 085 26	14.109 310 18
10^{3}	10^{-3}	1.569 863 463	4.707 893 531	7.846 262 981	10.984 681 08	14.123 115 57
5×10^{3}	0.5×10^{-3}	1.570 800 476	4.711 552 792	7.852 474 814	10.993 421 09	14.134 375 45
10^{4}	10^{-4}	1.570 702 922	4.711 939 009	7.853 209 047	10.994 483 94	14.135 760 44
5×10^{4}	0.5×10^{-4}	1.570 796 742	4.712 305 345	7.853 830 924	10.995 358 93	14.136 887 74
10^{5}	10^{-5}	1.570 786 985	4.712 343 979	7.853 904 368	10.995 465 24	14.137 026 28
5×10^{5}	0.5×10^{-5}	1.570 796 368	4.712 380 617	7.853 966 563	10.995 552 75	14.137 139 02
10^{6}	10^{-6}	1.570 795 393	4.712 384 480	7.853 973 907	10.995 563 38	14.137 152 87
Fixed-Free [5]		1.570 796 327	4.712 388 980	7.853 981 634	10.995 574 29	14.137 166 94

Case IV: Generally Constrained

The shaft shown in Fig. 12 is considered as the last study. In this case, shaft is constrained by concentrated rotary masses and rotary springs at both ends. Rotary inertia and spring constants are considered as $S_0 = S_1 = 1$ and $R_0 = R_1 = 1$. Boundary conditions of this shaft are assumed as the combination of the third and the fourth type of boundary conditions explained previously.

At $x = 0$

$$I_p G \left.\frac{\partial \theta(x,t)}{\partial x}\right|_{x=0} = K_{T0}\theta(0,t) + J_0 \left.\frac{\partial \theta(x,t)}{\partial t}\right|_{x=0}$$
$$\rightarrow \left(-K_{T0} + J_0\omega^2\right)\Phi(0) + \frac{I_p G}{l}\Phi'(0) = 0. \tag{41}$$

At $x = l$

$$I_p G \left.\frac{\partial \theta(x,t)}{\partial x}\right|_{x=l} = -\left(K_{T1}\theta(l,t) + J_1 \left.\frac{\partial \theta(x,t)}{\partial t}\right|_{x=l}\right)$$
$$\rightarrow \left(K_{T1} - J_1\omega^2\right)\Phi(0) + \frac{I_p G}{l}\Phi'(0) = 0. \tag{42}$$

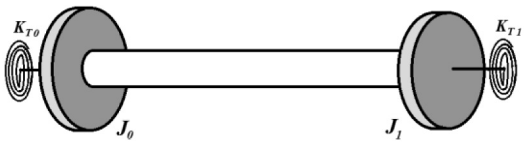

Fig. 12. Generally constrained shaft

Introducing Eq. (18) into Eq. (43) one can obtain

$$\begin{cases}(J_0\omega^2 - K_{T0})\,\Phi(0) + \frac{I_p G}{l}\Phi'(0) = 0,\\ (K_{T1} - J_1\omega^2)\sum_{k=0}^{n-1}\lambda^k\left(\frac{\Phi(0)}{(2k)!} + \frac{\Phi'(0)}{(2k+1)!}\right) + \frac{I_p G}{l}\left(\sum_{k=1}^{n-1}\lambda^k\frac{\Phi(0)}{(2k-1)!} + \sum_{k=0}^{n-1}\lambda^k\frac{\Phi'(0)}{(2k)!}\right) = 0.\end{cases} \tag{43}$$

Setting the determinant of coefficient matrix to zero gives us natural frequencies as presented in Table 8. Similarly to the previous cases, the mode shapes for this generally constrained shaft are also obtained and shown in Fig. 13

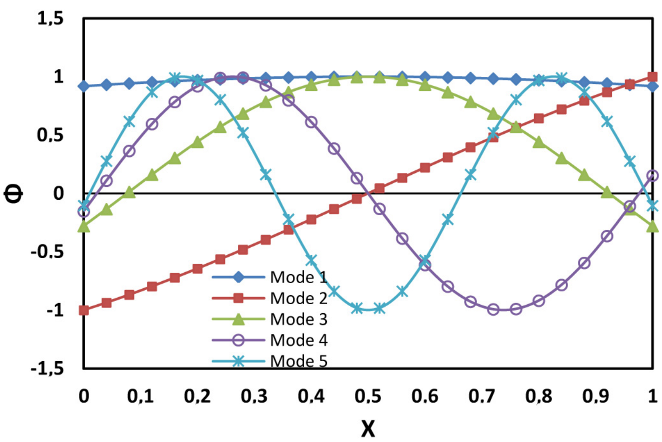

Fig. 13. The first five mode shapes of generally constrained shaft

Table 8. Five non-dimensional natural frequencies of generally constrained shaft

n	Ω_1	Ω_2	Ω_3	Ω_4	Ω_5
2	0.793 619 736	1.634 378 870	3.270 928 527		
3	0.809 185 553	1.589 227 829	–		
4	0.808 667 320	1.599 093 153	3.698 242 421		
5	0.808 675 143	1.598 370 798	3.706 180 184	5.437 343 359	
6	0.808 675 073	1.598 399 011	3.707 946 648	–	
7	0.808 675 073	1.598 398 314	3.707 693 808	6.338 181 866	
8	0.808 675 073	1.598 398 326	3.707 706 498	6.681 862 007	7.470 417 128
9	0.808 675 073	1.598 398 326	3.707 706 568	6.583 946 495	–
10	0.808 675 073	1.598 398 326	3.707 706 516	6.591 960 166	8.864 845 819
11	0.808 675 073	1.598 398 326	3.707 706 520	6.591 257 104	–
12	0.808 675 073	1.598 398 326	3.707 706 520	6.591 305 822	9.544 059 542
13	0.808 675 073	1.598 398 326	3.707 706 520	6.591 303 047	9.649 040 503
14	0.808 675 073	1.598 398 326	3.707 706 520	6.591 303 177	9.632 307 301
15	0.808 675 073	1.598 398 326	3.707 706 520	6.591 303 172	9.634 023 590
16	0.808 675 073	1.598 398 326	3.707 706 520	6.591 303 172	9.633 862 407
17	0.808 675 073	1.598 398 326	3.707 706 520	6.591 303 172	9.633 875 635
18	0.808 675 073	1.598 398 326	3.707 706 520	6.591 303 172	9.633 874 673
19	0.808 675 073	1.598 398 326	3.707 706 520	6.591 303 172	9.633 874 736
20	0.808 675 073	1.598 398 326	3.707 706 520	6.591 303 172	9.633 874 732
21	0.808 675 073	1.598 398 326	3.707 706 520	6.591 303 172	9.633 874 732
Rao [17]	0.808 675 000	1.598 398 000	3.707 706 000	6.591 303 000	9.633 881 000

Table 9. Effects of constraining elements on natural frequencies of symmetric shaft ($S_0 = S_1 = S$ and $R_0 = R_1 = R$)

S	R	Ω_1	Ω_2	Ω_3	Ω_4	Ω_5
	0.01	0.129 024 761	2.633 663 390	5.309 868 383	8.068 475 539	10.909 474 86
	0.1	0.405 894 299	2.686 702 614	5.332 783 174	8.080 573 095	10.916 402 66
0.1	1	1.219 177 805	3.147 512 538	5.562 954 151	8.205 151 964	10.987 831 09
	10	2.598 133 469	5.081 849 252	7.386 277 179	9.591 338 725	11.895 108 02
	100	3.079 43 4 356	6.155 403 267	9.223 825 855	12.279 174 58	15.313 098 83
	0.01	0.099 979 161	1.724 903 497	4.058 322 025	6.851 449 522	9.826 438 758
	0.1	0.315 567 184	1.762 544 655	4.065 614 364	6.853 368 829	9.827 140 902
0.5	1	0.978 635 977	2.099 863 563	4.142 011 418	6.873 157 684	9.834 286 651
	10	2.462 292 525	4.024 484 452	5.151 849 044	7.145 651 403	9.920 423 910
	100	3.077 016 670	6.132 420 568	9.115 391 499	11.819 229 67	13.590 946 30
	0.01	0.081 642 095	1.309 790 315	3.673 524 697	6.584 685 577	9.631 706 320
	0.1	0.257 958 997	1.338 660 707	3.676 510 505	6.585 276 544	9.631 901 674
1	1	0.808 675 073	1.598 398 326	3.707 706 52	6.591 303 172	9.633 874 732
	10	2.267 870 949	3.158 142 749	4.169 543 095	6.665 644 662	9.655 761 080
	100	3.073 730 117	6.090 170 862	8.724 369 604	9.883 854 288	10.698 666 63
	0.01	0.042 639 850	0.623 658 691	3.264 011 152	6.346 197 450	9.467 024 543
	0.1	0.134 830 671	0.637 465 266	3.264 210 361	6.346 225 330	9.467 032 989
5	1	0.426 103 068	0.761 880 222	3.266 235 894	6.346 505 473	9.467 117 638
	10	1.337 404 751	1.522 996 552	3.290 426 251	6.349 447 028	9.467 982 974
	100	3.029 713 914	4.399 942 998	4.586 972 882	6.404 900 879	9.479 045 146

$$\left|\begin{matrix} J_0\omega^2 - K_{T0} & \frac{I_pG}{l} \\ (K_{T1} - J_1\omega^2)\sum\limits_{k=0}^{n-1}\frac{\lambda^k}{(2k)!} + \frac{I_pG}{l}\sum\limits_{k=1}^{n-1}\frac{\lambda^k}{(2k-1)!} & \sum\limits_{k=0}^{n-1}\lambda^k\left(\frac{(K_{T1}-J_1\omega^2)}{(2k+1)!} + \frac{I_pG}{l}\frac{1}{(2k)!}\right)\end{matrix}\right| = 0. \quad (44)$$

In this case the effects of constraining elements (rotary springs and rotary mass) on natural frequencies of the shaft are also studied. Table 9 contains the results obtained for symmetric shaft. It is observed that by increasing spring constants at the ends, natural frequencies increase. But increasing the rotary inertia at the ends of the shaft leads to decreasing natural frequencies.

Table 10 shows the results obtained for asymmetric shaft. In this case, the values of rotary inertia at the ends are considered reverse of each other. It is also true about the spring constant. As displayed in Table 10 for certain values of rotary inertia, the natural frequencies of the shaft decrease with increasing constant R. On the other hand, for certain values of spring constants, the natural frequencies of the shaft increase with increasing constant S.

Table 10. Effects of constraining elements on natural frequencies of asymmetric shaft ($S = S_0 = 1/S_1$ and $R = R_0 = 1/R_1$)

S	R	Ω_1	Ω_2	Ω_3	Ω_4	Ω_5
0.1	1	0.029 652 592	1.896 667 610	4.489 986 380	7.317 278 810	10.247 980 79
	2	0.026 152 016	2.181 044 171	4.673 189 102	7.413 421 858	10.299 461 77
	5	0.024 612 950	2.600 365 446	5.142 114 709	7.728 773 053	10.477 190 55
	10	0.024 322 762	2.841 954 501	5.599 107 760	8.228 107 822	10.836 204 75
	100	0.024 214 367	3.110 383 811	6.218 681 166	9.323 087 575	12.420 597 58
0.5	1	0.066 248 190	1.494 648 846	3.705 783 061	6.591 570 862	9.634 148 690
	2	0.058 440 110	1.790 577 029	3.776 796 030	6.605 388 629	9.638 611 339
	5	0.055 009 470	2.340 314 399	4.046 146 476	6.653 975 606	9.653 137 785
	10	0.054 363 676	2.731 717 161	4.593 670 479	6.766 873 847	9.681 881 975
	100	0.054 123 601	3.109 868 160	6.206 930 223	9.264 214 999	12.135 278 62
1	1	0.093 557 196	1.209 762 638	3.449 785 796	6.441 842 420	9.531 085 592
	2	0.082 568 277	1.468 544 527	3.475 353 387	6.445 663 561	9.532 252 611
	5	0.077 745 028	2.013 272 451	3.574 145 780	6.458 242 426	9.535 909 139
	10	0.076 839 203	2.530 651 855	3.830 079 762	6.483 762 899	9.542 574 442
	100	0.076 504 580	3.109 074 636	6.184 322 062	8.987 945 241	10.368 963 74
5	1	0.203 757 518	0.626 812 532	3.214 109 687	6.319 624 160	9.449 092 270
	2	0.182 081 844	0.757 316 830	3.215 339 284	6.319 782 254	9.449 139 349
	5	0.172 689 534	1.061 338 263	3.219 355 251	6.320 270 289	9.449 283 090
	10	0.170 982 734	1.430 525 860	3.227 231 812	6.321 118 809	9.449 527 433
	100	0.170 396 524	3.091 912 856	4.494 970 135	6.350 207 540	9.455 120 609
10	1	0.263 075 602	0.491 144 462	3.191 700 677	6.308 384 728	9.441 595 640
	2	0.247 879 358	0.562 969 164	3.191 959 672	6.308 417 857	9.441 605 498
	5	0.241 147 240	0.769 956 058	3.192 900 164	6.308 534 865	9.441 640 130
	10	0.240 056 243	1.034 296 495	3.194 645 408	6.308 739 469	9.441 700 025
	100	0.239 795 916	2.944 060 849	3.386 024 762	6.313 612 630	9.442 914 827

4. Conclusion

In this study a new approach called Adomian Decomposition Method was employed to solve torsional vibration problems of shafts. Obtained results indicate that present analysis is completely accurate, and provides a unified and systematic procedure which is simple and more straightforward than other methods. Other approximate approaches such as Rayleigh-Ritz method or Galerkin method may also be applicable to such cases. However, it may be difficult to determine higher natural frequencies and mode shapes on account of not choosing complete and correct admissible functions. In particular, the Adomian method provides immediate and visible symbolic terms of analytic solutions, as well as numerical solutions of the differential equations without linearisation or discretisation. Using ADM, the governing differential equation becomes a recursive algebraic equation and boundary conditions become simple algebraic frequency equations which are suitable for symbolic computation. Moreover, after some simple algebraic operations on these frequency equations, any ith natural frequency and the closed form series solution of any ith mode shape can be obtained. The most brilliant aspect of this method is that arbitrary order of accuracy is achievable by choosing proper truncation value for series. Parametric study of various cases showed that increasing the spring constants at the ends of the constrained shafts, the natural frequencies increase and that increasing the rotary inertia at the ends of the shaft leads to decreasing natural frequencies.

References

[1] Bernasconi, O., Solution for torsional vibrations of stepped shafts using singularity functions, International Journal of Mechanical Science 28 (1) (1986) 31–39.

[2] Zajaczkowski, J., Torsional vibration of shafts coupled by mechanisms, Journal of Sound and Vibration 116 (2) (1987) 221–237.

[3] Rao, M. A., Srinivas, J., Raju, V. B. V., Kumar, K. V. S. S., Coupled torsional-lateral vibration analysis of geared shaft systems using mode synthesis, Journal of Sound and Vibration 261 (2) (2003) 359–364.

[4] Chen, D. W., An exact solution for free torsional vibration of a uniform circular shaft carrying multiple concentrated elements, Journal of Sound and Vibration 291 (3–5) (2006) 627–643.

[5] Gorman, D. J., Free Vibration Analysis of Beams and Shafts, Wiley, New York, 1975.

[6] Wu, J. S., Chen, C. H., Tortional vibration analysis of gear-branched systems by finite element method, Journal of Sound and vibration 240 (1) (2001) 159–182.

[7] Adomian, G., A review of the decomposition method in applied mathematics, Journal of Mathematical Analysis and Applications 135 (2) (1988) 501–544.

[8] Adomian, G., A review of the decomposition method and some recent results for nonlinear equation, Mathematical and Computer Modeling 13 (7) (1990) 17–43.

[9] Adomian, G., SolvingFrontier problems of Physics: The decomposition method. Kluwer Academic Publishers, 1994.

[10] Adomian, G., Rach, R., Modified decomposition solution of linear and nonlinear boundary-value problems, Nonlinear Analysis Theory Methods & Applications 23 (5) (1994) 615–619.

[11] Wazwaz, A. M., A reliable modification of Adomian decomposition method, Applied Mathematics and Computation 102 (1) (1999) 77–86.

[12] Wazwaz, A. M., El-Seyed, S. M., A new modification of the Adomian decomposition method for linear and nonlinear operators, Applied Mathematics and Computation 122 (3) (2001) 393–405.

[13] Babolian, E., Biazar, J., Solution of nonlinear equations by modified Adomian decomposition method, Applied Mathematics and Computation 132 (1) (2002) 167–172.

[14] Pamuk, S., An application for linear and nonlinear heat equations by Adomian decomposition method, Applied Mathematics and Computation 163 (1) (2005) 89–96.

[15] Lai, H. Y., Hsu, J. C., Chen, C. K., An innovative eigenvalue problem solver for free vibration of Euler-Bernoulli beam by using the Adomian decomposition method, Computers and Mathematics with Applications 56 (12) (2008) 3 204–3 220.

[16] Farshidianfar, A., Tabassian, R., Khoee, O. K., Noei, S. J., Solving Free Vibration of Stepped Beam by Using the Adomian Decomposition Method, Proceedings of the ASME 2020 10th Biennial Conference on Engineering Systems Design and Analysis, Istanbul, ASME, 2010, 263–270.

[17] Rao, C. K., Torsional frequencies and mode shapes of generally constrained shafts and piping, Journal of sound and vibration 125 (1) (1988) 111–121.